Image potential for a tunneling electron

Pedro M. Echenique
Cavendish Laboratory, Madingley Road, Cambridge CB3 0HE, United Kingdom
and Euskal Herriko Unibertsitatea, Kimika Fakultatea, Donostia, Euskadi, Spain

Alberto Gras-Marti
Laboratori de Capes Fines i Collisions Atómiques i Sólids (L.C.F.C.A.S.), Departament de Física Aplicada, Facultat de Ciències, Universitat d'Alacant, Apt. 99, E-03080 Alacant, Spain
and Health and Safety Research Division, Oak Ridge National Laboratory, Oak Ridge, Tennessee 37831-6123
and University of Tennessee, Knoxville, Tennessee 37996

J. Richard Manson
Department of Physics and Astronomy, Clemson University, Clemson, South Carolina 29634

Rufus H. Ritchie
Health and Safety Research Division, Oak Ridge National Laboratory, Oak Ridge, Tennessee 37831-6123
and University of Tennessee, Knoxville, Tennessee 37996
(Received 20 November 1986)

The image potential appropriate to an electron tunneling from a metal into the conduction band of an insulator is calculated with the many-body self-energy formalism developed by Manson and Ritchie [Phys. Rev. B **24**, 4867 (1981)]. Analytical results are derived for a simple but complete basis set of eigenfunctions of the one-electron potential experienced by the electron in the noninteracting system. The dynamical corrections to the classical image potential are analyzed.

I. INTRODUCTION

The analysis of electron tunneling from a metal, through a classically forbidden region, into vacuum or into the conduction band of an insulator is of central importance in processes leading to dielectric breakdown. Current phenomenological theory of such tunneling uses classical image theory reduced by the static dielectric function of the insulator in representing the potential seen by a tunneling electron.[1]

The interaction potential between a charged particle and a semi-infinite polarizable medium has been investigated within classical, semiclassical, and quantum-mechanical frameworks. A short discussion of self-energy calculations prior to about 1981 is given in Refs. 2 and 3. These studies are important for the interpretation of the results obtained with various electron-based surface spectroscopies, including low-energy electron diffraction (LEED) and electron-energy-loss spectroscopies as reflection techniques (REEL) or as scanning transmission microscopy (STEM). A detailed knowledge of the attractive potential is important also for the analysis of bound-state formation in the electron-surface interaction.[4] In a situation where an electron tunnels through a classically forbidden region one needs a quantum-mechanical description of both the dynamics of the surface excitations and the dynamics of the electron. For particle positions close to the surface of the medium with which it interacts, one cannot neglect the change in the perpendicular component of the particle motion due to the exchange of virtual excitations with the many-body system.[2] Jonson[3] investigated also the dynamical image potential appropriate for tunneling electrons (through a rectangular barrier) by way of the Green's-function formalism, for a square-well potential. The formalism in Ref. 2, which will be used in this paper, includes full three-dimensional recoil effects, and has been applied recently to investigate particle-surface interactions by neutral particles,[5] and also to a reevaluation of the van der Waals forces between two atoms.[6] Comparison with the results of Jonson[3] will be made.

We shall employ here modern many-body theory[2] to study the image potential appropriate to a tunneling electron, and shall calculate the self-energy of the tunneling electron due to its binding with its image potential. The self-energy depends significantly on the dynamical response of the electronic system near the metal surface. In order to obtain fully analytic results, a complete orthogonal electron basis set appropriate to an artificial one-electron potential near the metal surface has been uti-

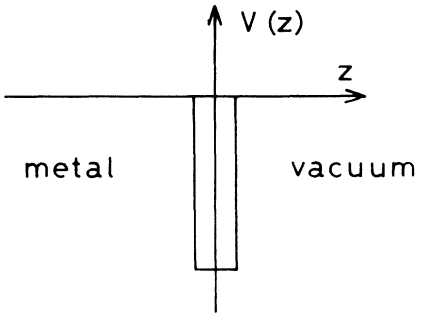

FIG. 1. Geometry of the system. The plane $z=0$ locates the interface between the metal ($z<0$) and the vacuum ($z>0$). The potential-energy barrier $V(z)$ seen by the electron will be modeled as a δ function in this paper.

lized to obtain the complex, spatially dependent self-energy in this region. This self-energy is a generalization of the classical image potential and includes dissipative effects as well as the effect of virtual surface and virtual bulk excitations. In our application, we have described the binding with a δ-function potential, for which the corresponding basis set has the simplest form after the momentum eigenfunctions set.

The outline of this paper is as follows. In Sec. II we briefly sketch the self-energy formalism, which is then applied to an electron interacting with a many-body target. The resulting self-energy and energy shift, obtained for a δ-function interaction, are given in Sec. III. Some results are evaluated and discussed in Sec. IV.

II. SELF-ENERGY CALCULATION

A. The general formalism

Manson and Ritchie have presented[2] a general expression for the space-dependent, complex self-energy of an electron in a given state interacting with a specified N-particle target. The quantal self-energy was obtained from an exact solution of second-order perturbation theory including full three-dimensional recoil effects. For an electron with energy $\mathscr{E}_i$ in an initial state defined by an eigenfunction $\phi_i(\mathbf{r})$, the space-dependent self-energy is defined as

$$\Sigma_i(\mathbf{r})=\sum_\alpha\sum_\beta \frac{\phi_\alpha(\mathbf{r})}{\phi_i(\mathbf{r})}\frac{\langle i0\,|\,H'\,|\,\alpha\beta\rangle\langle\psi_\beta\,|\,H'\,|\,\psi_0\rangle}{\mathscr{E}_i+E_0-\mathscr{E}_\alpha-E_\beta+i\delta}\ , \tag{1}$$

where $|\,\psi_\beta\rangle$ is the exact state vector of the target in its β-excited state with energy E_β, and $|\,\phi_\alpha\rangle$ is the electron state vector when it has the energy $\mathscr{E}_\alpha$. The state vector of the noninteracting system is $|\,\alpha\beta\rangle=|\,\phi_\alpha\rangle\,|\,\psi_\beta\rangle$, and H' is the interaction energy. δ is a positive infinitesimal. The result in Eq. (1) is the lowest-order nonvanishing contribution to $\Sigma_i(\mathbf{r})$. Extension to higher order in perturbation theory is immediate.

The shift in the energy of the electron in the $|\,\phi_i\rangle$ state is then given by the ground-state expectation value of the space-dependent self-energy

$$\Delta E_i=\int \phi_i^*(\mathbf{r})\Sigma_i(\mathbf{r})\phi_i(\mathbf{r})d\mathbf{r}\ . \tag{2}$$

Note that Eq. (2) gives the self-energy times the probability of finding the particle in the initial state, integrated over position.

To obtain an accurate expression for the self-energy we need both a good description of the interacting potential, i.e., the screened electron-target interaction, and an appropriate orthonormal basis set describing the system under consideration in the absence of any coupling of the electron to the many-body target.

B. Self-energy of a tunneling electron

Take an electron, in vacuum, at a distance $z>0$ from a metal surface; see Fig. 1. Let $V(z)$ be the "one-electron" potential experienced by the electron, neglecting the image potential. Then, an arbitrary state of the electron in interaction with the potential that is originated by its own presence near the surface, can be expanded in terms of the complete orthonormal set that is generated by the Schrödinger equation,

$$-\frac{\hbar^2\nabla^2}{2m}\phi_n+V(z)\phi_n=\mathscr{E}_n\phi_n\ , \tag{3}$$

m is the electron mass. Since there is translational invariance parallel to the surface of the medium, the wave functions ϕ_n will be written as the product of plane waves in the transverse coordinates $\boldsymbol{\rho}=(x,y)$, modulated by functions $u_n(z)$ of the perpendicular coordinate, z; see Eqs. (7) and (8) below.

We assume that the dynamical properties of the metal, which is located in the half-space $z<0$, may be codified in a surface-plasmon field[7] whose interaction with an electron at the point $\mathbf{r}=(\boldsymbol{\rho},z)$ is represented by the Hamiltonian

$$H_{\rm sp}=\sum_{\boldsymbol{\kappa}}\alpha_\kappa e^{i\boldsymbol{\kappa}\cdot\boldsymbol{\rho}-\kappa|z|}(b_{\boldsymbol{\kappa}}+b^\dagger_{-\boldsymbol{\kappa}})\ , \tag{4}$$

where $\boldsymbol{\kappa}$ is the wave vector of a surface plasmon with energy $\hbar\omega_{s\kappa}$, and the annihilation ($b_{\boldsymbol{\kappa}}$) and creation ($b^\dagger_{-\boldsymbol{\kappa}}$) operators for the surface plasmons obey the following commutation relations:

$$[\,b_{\boldsymbol{\kappa}},b^\dagger_{\boldsymbol{\kappa}'}]=\delta_{\boldsymbol{\kappa},\boldsymbol{\kappa}'}\ . \tag{5}$$

The coupling coefficient in Eq. (4) is[8]

$$\alpha_\kappa=\left[\frac{\pi e^2\hbar\omega_s^2}{A\kappa\omega_{s\kappa}}\right]^{1/2}\ , \tag{6}$$

where $\omega_s=\lim_{\kappa\to 0}\omega_{s\kappa}$, and A is the area of the surface. For many purposes it is sufficient to take the dispersionless limit $\omega_{s\kappa}=\omega_s=\omega_p/\sqrt{2}$, where $\omega_p=(4\pi n_0e^2/m)^{1/2}$ is the volume-plasmon frequency of an electron gas of density n_0.

The initial-state vector to be introduced in Eq. (1),

$$|\,0i\rangle=\frac{e^{i\mathbf{P}_i\boldsymbol{\rho}}}{\sqrt{A}}u_i(z)\,|\,0\rangle\ , \tag{7}$$

represents a noninteracting electron surface-plasmon field ket. $\hbar\mathbf{P}_i$ is the momentum, perpendicular to the z axis, of the electron in its "initial" state, and $|\,0\rangle$ is the ground-state ket vector of the surface-plasmon field. Similarly, the intermediate-state vector, $|\,\alpha\beta\rangle$ in Eq. (1), which we write as

$$|\,\alpha\beta\rangle=\frac{e^{i\mathbf{P}\boldsymbol{\rho}}}{\sqrt{A}}u_n(z)b^\dagger_{\boldsymbol{\kappa}}\,|\,0\rangle\ , \tag{8}$$

represents a virtual state in which the electron makes a transition to the state characterized by the momentum $\hbar\mathbf{P}$ parallel to the surface and the excitation quantum number n, with a total electron energy $\mathscr{E}_n=\hbar^2P^2/2m+\varepsilon_n$. ε_n is the eigenenergy corresponding to the state $u_n(z)$. The surface-plasmon field is excited to a state with momentum $\hbar\boldsymbol{\kappa}$.

Calculating the matrix elements in Eq. (1), and carrying out the sum over $\mathbf{P}$, one obtains for the z-dependent self-energy

$$\Sigma_i(z)=\sum_n\sum_\kappa \alpha_\kappa^2 e^{-\kappa|z|}\frac{u_n(z)}{u_i(z)}\frac{\int dz' u_i(z')e^{-\kappa|z'|}u_n^*(z')}{\varepsilon_i-\varepsilon_n+\frac{\hbar^2}{2m}(P_i^2-[\mathbf{P}_i-\boldsymbol{\kappa}]^2)-\hbar\omega_{s\kappa}+i\delta}\ . \tag{9}$$

Since the system is translationally invariant in the x and y coordinates, the energy shift of a given state i, Eq. (2), reduces to

$$\Delta E_i=\int dz\, u_i^*(z)\Sigma_i(z)u_i(z)\ , \tag{2'}$$

and, introducing the result in Eq. (9),

$$\Delta E_i=\sum_n\sum_\kappa \alpha_\kappa^2\frac{\left|\int dz\, u_i(z)e^{-\kappa|z|}u_n^*(z)\right|^2}{\varepsilon_i-\varepsilon_n+\frac{\hbar^2}{2m}(P_i^2-[\mathbf{P}_i-\boldsymbol{\kappa}]^2)-\hbar\omega_{s\kappa}+i\delta}\ . \tag{10}$$

So far, the one-electron potential in Eq. (3) has not been specified. A constant potential, and the corresponding plane-wave set, was taken in Ref. 2 for the calculation of the self-energy.

III. APPLICATION: δ-FUNCTION POTENTIAL

The treatment presented above will be applied here to the calculation of the self-energy of an electron initially in the bound state of a one-dimensional δ-function potential. The case of an electron initially in a continuum state will be considered at the end of Sec. III.

One would ideally like to consider eigenfunctions of the one-dimensional Schrödinger equation (3) with a potential $V(z)$ taken from a density-functional calculation. This potential would include the static image potential for $z\to\infty$. A more modest calculation would use a step function for $V(z)$, along similar lines as in Jonson's work.[3] Even these eigenfunctions give integrals in Eq. (9) that are rather intricate. In order to obtain fully analytic results, we now apply the results obtained for the energy shift and the self-energy to the set of eigenfunctions obtained when the δ-function potential energy, $V(z)=-(\hbar^2\lambda_0/m)\delta(z)$, is inserted in Eq. (3); see Fig. 2. The complete and orthogonal basis set consists of a bound state,

$$u_0(z)=(\lambda_0)^{1/2}e^{-\lambda_0|z|}\ , \tag{11}$$

and two states in the continuum, corresponding to traveling wave eigenfunctions directed towards $\pm z$,

$$u_\lambda^{(1)}(z)=\frac{1}{\sqrt{2\pi}}\left[\left[e^{\pm i\lambda z}+\frac{i\lambda_0}{\lambda-i\lambda_0}e^{\mp i\lambda z}\right]\Theta(\mp z)+\frac{\lambda}{\lambda-i\lambda_0}e^{\pm i\lambda z}\Theta(\pm z)\right]\ , \tag{12}$$

which can also be expressed in terms of the transmitted and reflected waves; see Fig. 2. $\Theta(z)$ is the unit step function. Alternatively, the continuum states can also be expressed as standing waves of odd or even parity, i.e., $\sin(\lambda z)$ and $\cos(\lambda z)$, but the above representation of traveling wave eigenfunctions is more convenient. The binding energy of the single discrete state is $\varepsilon_0=-\hbar^2\lambda_0^2/2m$, and the continuum states have energies $\varepsilon_\lambda=\hbar^2\lambda^2/2m$ relative to the vacuum. The closure relation is satisfied,

$$u_0(z)u_0^*(z')+\sum_{i=1}^{2}\int_0^\infty d\lambda\, u_\lambda^{(i)}(z)u_\lambda^{(i)*}(z')=\delta(z-z')\ . \tag{13}$$

When the initial state of the electron coincides with the bound state of the δ-function potential, the two matrix elements appearing in Eq. (9) are

$$\langle u_0\,|\,e^{-\kappa|z|}\,|\,u_0\rangle=\frac{2\lambda_0}{2\lambda_0+\kappa}\ , \tag{14}$$

and

$$\langle u_0\,|\,e^{-\kappa|z|}\,|\,u_\lambda\rangle=\left[\frac{\lambda_0}{2\pi}\right]^{1/2}\frac{2\lambda\kappa}{(\lambda-i\lambda_0)[\lambda^2+(\lambda_0+\kappa)^2]}\ , \tag{15}$$

the result for the two states $u_\lambda^{(1)}$ and $u_\lambda^{(2)}$ being the same.

A. Self-energy

We now examine Eq. (9). We are only interested[7] in the self-energy of an electron in vacuum, i.e., in the region $z>0$. The term with $\kappa=0$ and $n=0$ should be excluded from the summation in Eq. (9). However, since in the limit $A\to\infty$ the sum over κ will become an integration over κ, the case $\kappa=0$ is automatically excluded, and the

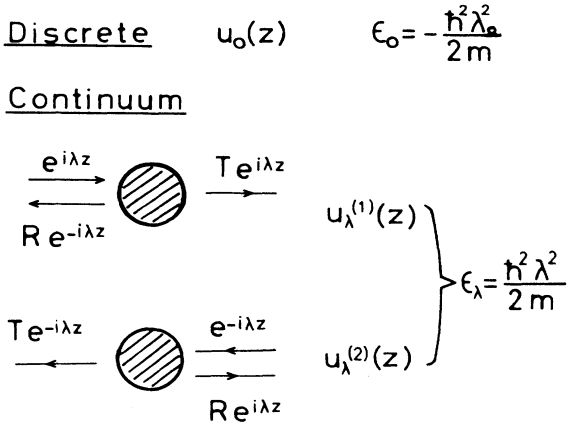

FIG. 2. Orthonormal basis set of the δ-function potential described in the text; R and T are the amplitudes for the reflected and transmitted waves, respectively, for electrons incident from the left and right, with $R=i\lambda_0/(\lambda-i\lambda_0)$, $T=\lambda/(\lambda-i\lambda_0)$. The wave functions u_0, $u_\lambda^{(1)}$, and $u_\lambda^{(2)}$ are given in Eqs. (11) and (12).

contribution from the $n=0$ term must also be considered. Using the results in Eqs. (14) and (15), we can write the self-energy for the state at the bottom of the band,

$$\Sigma_0(z)=\Sigma_{00}(z)+\Sigma_{0\lambda}(z)\ , \tag{16}$$

where we have separated the contributions to the self-energy originated from transitions with no change (00) of the state in the direction normal to the surface, from those in which the electron state associated with the normal motion changes, (0λ). For arbitrary initial velocity parallel to the surface, $\mathbf{v}_{||}=\hbar\mathbf{P}_0/m$, the contributions to the self-energy as seen by a charge in the bound state are

$$\Sigma_{00}(z)=-\frac{me^2\omega_s^2\lambda_0}{\pi\hbar}\int\frac{d^2\kappa}{\kappa\omega_{s\kappa}}\frac{e^{-\kappa z}}{(2\lambda_0+\kappa)[(\mathbf{P}_0-\boldsymbol{\kappa})^2-P_0^2+2m\omega_{s\kappa}/\hbar-i\delta]} \tag{17}$$

and

$$\Sigma_{0\lambda}(z)=-\frac{me^2\omega_s^2e^{\lambda_0 z}}{\pi^2\hbar}\int d^2\kappa\frac{e^{-\kappa z}}{\omega_{s\kappa}}I(\kappa)\ , \tag{18}$$

where

$$I(\kappa)=\int_0^\infty d\lambda\,\lambda\frac{\lambda\cos(\lambda z)-\lambda_0\sin(\lambda z)}{(\lambda^2+\lambda_0^2)[\lambda^2+(\lambda_0+\kappa)^2][\lambda^2+\lambda_0^2+(\mathbf{P}_0-\boldsymbol{\kappa})^2-P_0^2+2m\omega_{s\kappa}/\hbar-i\delta]}\ . \tag{19}$$

The integral $I(\kappa)$ decreases faster than $\exp(-\lambda_0 z)$ (see the Appendix), so that the contribution $\Sigma_{0\lambda}(z)$ is well behaved for $z\to\infty$.

The effect of using closure in the derivation of the self-energy $\Sigma_0(z)$ can be investigated. An upper limit to the self-energy can be obtained by neglecting the energy difference $\varepsilon_i-\varepsilon_n$ in the denominator in Eq. (9), and using the closure relation (13) to sum over intermediate states in Eq. (9), one obtains

$$\Sigma_0^c(z)=-\frac{me^2\omega_s^2}{2\pi\hbar}\int\frac{d^2\kappa}{\kappa\omega_{s\kappa}}\frac{e^{-2\kappa z}}{(\mathbf{P}_0-\boldsymbol{\kappa})^2-P_0^2+2m\omega_{s\kappa}/\hbar-i\delta}\ , \tag{20}$$

which is independent of λ_0, i.e., of the strength of the δ potential interaction.

Often, in deriving explicit expressions in the following, we shall take the initial electron state to have zero momentum parallel to the surface, and shall let $\mathbf{P}_0=\mathbf{0}$. Also, the dispersionless limit $\omega_{s\kappa}\to\omega_s$ will usually be taken. From Eqs. (16)–(19), and from the expression given in the Appendix, one finds that the term Σ_{00} cancels out with one term of $\Sigma_{0\lambda}$, and then

$$\Sigma_0(z)=-\frac{me^2\omega_s}{2\hbar}\int_0^\infty d\kappa\frac{e^{-2\kappa z}}{m\omega_s/\hbar-\lambda_0\kappa}\left[1-\frac{\kappa\exp-\{[(2m\omega_s/\hbar+\kappa^2+\lambda_0^2)^{1/2}-\lambda_0-\kappa]z\}}{(2m\omega_s/\hbar+\kappa^2+\lambda_0^2)^{1/2}-\lambda_0}\right]\ . \tag{16'}$$

The first term inside the brackets in this expression gives the classical self-energy image potential (see below), whereas the second term in Eq. (16′) is due to recoil of the tunneling electron; this term decays exponentially away from the surface. At the singular point $m\omega_s/\hbar=\lambda_0\kappa$ the integrand in Eq. (16′) cancels and, as one expects for $\mathbf{P}_0=0$, there is no imaginary part of Σ_0. The saturation value of $\Sigma_0(z)$ at the surface can be easily calculated and is finite due to the presence of the recoil term in Eq. (16′). We only quote the limit for $\lambda_0\to 0$,

$$\Sigma_0(0)=-\frac{e}{2}\left[\frac{2m\omega_s}{\hbar}\right]^{1/2}\ ,$$

which coincides with a result derived in Ref. 5 for a charge near a surface and differs from previously obtained limits which did not include the full three-dimensional recoil.

Asymptotic expressions of the quantities in Eqs. (16)–(20) yield the expected results. In the limit of large z, only small values of κ contribute to the integrals and, letting $\kappa\to 0$ everywhere except in the exponential factors in the integrand, one gets

$$\Sigma_{00}(z)\simeq-\frac{e^2}{2z}\ , \tag{21a}$$

$$\Sigma_{0\lambda}(z)\simeq+\frac{e^2}{4z}\ , \tag{21b}$$

$$\Sigma_0^c(z)\simeq-\frac{e^2}{4z}\ . \tag{21c}$$

Therefore, both the exact expression for the self-energy and the one obtained using closure tend towards the well-known classical image potential at large distances from the surface, $-e^2/4z$, for any value of the strength, λ_0, of

the δ-function potential. The next contribution to $\Sigma_0(z)=\Sigma_{00}+\Sigma_{0\lambda}$ is $-e^2\lambda_0/4z^2$. Let us now discuss these results in relation with Jonson's work.[3] The self-energy obtained in Ref. 3, when the electron is inside a rectangular barrier [Eq. (20b) in Ref. 3] is identical with the first term in Eq. (16′) for the self-energy of an electron initially in a bound state. However, since Jonson's calculation does not include the recoil terms, he extracts both a real part of $\Sigma_0(z)$, which coincides with our results, and an imaginary part of $\Sigma_0(z)$, which appears to be spurious. We have found that, for $\mathbf{P}_0=0$, Σ_{00} is canceled by one term of $\Sigma_{0\lambda}$, and there is no imaginary part of $\Sigma_0(z)$. [See also the discussion after Eq. (33b) below.]

Equation (20) gives the semiclassical point particle result, including the recoil momentum $\hbar\kappa$. Note that there is some ambiguity in the use of the closure relation. One could replace $\varepsilon_i-\varepsilon_n$ in the denominator in Eq. (9) by an average value $-\hbar a$, and the asymptotic result in Eq. (21c) would become instead

$$\Sigma_0^c(z)\simeq-\frac{\omega_s}{\omega_s+a}\frac{e^2}{4z}\ , \tag{21c'}$$

which coincides with the one in Eq. (21c) for $\hbar a \ll \hbar\omega_s$.

B. Energy shift

The energy shift is also a quantity of interest and one can, for instance, derive from it the effective mass of the electron. We consider first the case of the electron initially in the bound state. From the results in Eqs. (10), (14), and (15), and splitting up the two contributions to the sum over the final electron states, like the case of the self-energy, we write [cf. Eq. (16)],

$$\Delta E_0=\Delta E_{00}+\Delta E_{0\lambda} \tag{22}$$

where ΔE_{00} corresponds to the $n=0$ term and $\Delta E_{0\lambda}$ to the remaining terms in Eq. (10), with

$$\Delta E_{00}=-\frac{2me^2\omega_s^2\lambda_0^2}{\pi\hbar}\int\frac{d^2\kappa}{\omega_{s\kappa}\kappa}\frac{1}{(2\lambda_0+\kappa)^2[(\mathbf{P}_0-\boldsymbol{\kappa})^2-P_0^2+2m\omega_{s\kappa}/\hbar-i\delta]} \tag{23}$$

and

$$\Delta E_{0\lambda}=-\frac{me^2\omega_s^2\lambda_0}{\pi^2\hbar}\int d^2\kappa\frac{\kappa}{\omega_{s\kappa}}\int_0^\infty d\lambda\,\lambda^2\frac{1}{(\lambda^2+\lambda_0^2)[\lambda^2+(\lambda_0+\kappa)^2]^2[\lambda^2+\lambda_0^2+(\mathbf{P}_0-\boldsymbol{\kappa})^2-P_0^2+2m\omega_{s\kappa}/\hbar-i\delta]}\ . \tag{24}$$

Let us calculate the self-energy in the limit of a deep bound state, $\lambda_0\to\infty$. The contribution $\Delta E_{0\lambda}$ vanishes, and from Eq. (23) one gets, for $\mathbf{P}_0=0$ and $\omega_{s\kappa}=\omega_s$,

$$\Delta E_0=-\frac{\pi e^2}{2}\left[\frac{m\omega_s}{2\hbar}\right]^{1/2}\ , \tag{25}$$

which reproduces the Evans and Mills[4] limit for a classical point particle. The limit $\lambda_0\to\infty$ is therefore equivalent to taking an electron located in a well-defined position.

Although the calculation of the energy shift is exact it is useful to investigate, in the analytically simple case of the basis set of the δ-function potential, which is the effect of invoking closure in an approximate evaluation of the energy shift. Following in the expression in Eq. (10), the procedure that led to Eq. (20), yields

$$\Delta E_0^c=-\frac{me^2\omega_s^2\lambda_0}{2\pi\hbar}\int\frac{d^2\kappa}{\kappa\omega_{s\kappa}}\frac{1}{(\lambda_0+\kappa)[(\mathbf{P}_0-\boldsymbol{\kappa})^2-P_0^2+2m\omega_{s\kappa}/\hbar-i\delta]}\ . \tag{26}$$

In contrast to the corresponding result obtained for the self-energy, Eq. (20), the energy shift depends upon the strength of the potential, λ_0. For large λ_0, the expression for the energy shift obtained using the closure relation coincides with the exact result in Eq. (22). In the limit $\lambda_0\to 0$, the expressions for the energy shifts in Eqs. (22) to (26) cancel out.

Another approximation in the evaluation of the energy shift was used by Nieminen and Hodges,[10] who neglected ε_n for $n>0$ in Eq. (10). One gets

$$\Delta E_0^{\mathrm{NH}}=-\frac{me^2\omega_s^2}{2\pi\hbar}\int\frac{d^2\kappa}{\kappa\omega_{s\kappa}}\frac{1}{\lambda_0^2+(\mathbf{P}_0-\boldsymbol{\kappa})^2-P_0^2+2m\omega_{s\kappa}/\hbar-i\delta}\left[\frac{\lambda_0}{\lambda_0+\kappa}-\left[\frac{2\lambda_0}{2\lambda_0+\kappa}\right]^2\right]\ , \tag{27}$$

a results that should be compared with those in Eqs. (22) and (26). When $\mathbf{P}_0\neq 0$, one may look for the contribution of the surface plasmon field to the effective mass of the bound electron. This is of current interest in the theory of image-potential-induced states in solids. The effective mass for the tunneling electron can be calculated from the energy shift. Expanding the integrand in Eq. (26) for small $\mathbf{P}_0$, we write

$$\Delta E_0^c=\Delta E_0^c(\mathbf{P}_0=0)+\delta\frac{\hbar^2P_0^2}{2m}\ , \tag{28}$$

where

$$\Delta E_0^c(\mathbf{P}_0=0)=-\frac{me^2\omega_s^2\lambda_0}{\hbar}\int_0^\infty \frac{d\kappa}{\omega_{s\kappa}}\frac{1}{(\lambda_0+\kappa)(\kappa^2+2m\omega_{s\kappa}/\hbar)} \tag{29}$$

and

$$\delta=-\frac{4m^2e^2\omega_s^2\lambda_0}{\hbar^3}\int_0^\infty \frac{d\kappa}{\omega_{s\kappa}}\frac{\kappa^2}{(\lambda_0+\kappa)(\kappa^2+2m\omega_{s\kappa}/\hbar)^3} . \tag{30}$$

The effective mass is then

$$m^*=\frac{m}{1+\delta}\simeq m(1-\delta) , \tag{31}$$

which, for large λ_0 and for $\omega_{s\kappa}=\omega_s$, becomes

$$\frac{\Delta m^*}{m}=-\delta=\frac{\pi e^2}{8}\left[\frac{m}{2\omega_s\hbar^3}\right]^{1/2} . \tag{31'}$$

The effective mass correction decreases with increasing ω_s or with decreasing electron gas density, a fact that has been pointed out recently in theoretical studies of effective masses of image-potential-induced surface states.[10]

C. Semiclassical force

Let us calculate the real and the imaginary parts of the self-energies given in Eqs. (17) and (20). The solutions, of course, will have two regimes, depending upon whether or not the particle has sufficient energy to generate a surface excitation.

Take the real part of the first contribution to the exact self-energy given by Eq. (17),

$$\mathrm{Re}\Sigma_{00}(z)=-\frac{2me^2\omega_s^2\lambda_0}{\hbar}\int_0^\infty \frac{d\kappa}{\omega_{s\kappa}}\frac{e^{-\kappa z}\Theta(\beta)}{(2\lambda_0+\kappa)\sqrt{\beta}} , \tag{32}$$

where $\Theta(\beta)$ is the unit step function and

$$\beta=\left[\kappa^2+\frac{2m\omega_{s\kappa}}{\hbar}\right]^2-(2\kappa P_0)^2 . \tag{32'}$$

From the result obtained using the closure relation, Eq. (20), one gets

$$\mathrm{Re}\Sigma_0^c(z)=-\frac{me^2\omega_s^2}{\hbar}\int_0^\infty \frac{d\kappa}{\omega_{s\kappa}}\frac{e^{-2\kappa z}\Theta(\beta)}{\sqrt{\beta}} , \tag{33a}$$

which, except for the factor 2 in the argument of the exponential, coincides with the exact result in Eq. (32) for large λ_0. Similarly,

$$\mathrm{Im}\Sigma_0^c(z)=-\frac{me^2\omega_s^2}{\hbar}\int_0^\infty \frac{d\kappa}{\omega_{s\kappa}}\frac{e^{-2\kappa z}\Theta(-\beta)}{\sqrt{-\beta}} . \tag{33b}$$

The last result is identical, except for the presence in β of the two-dimensional recoil term $\kappa^2/2$, to the result in Eq. (36) of Echenique *et al.*,[11] and leads, for large z and undispersed plasmons, to the result first derived by Echenique and Pendry,[12]

$$\mathrm{Im}\Sigma_0^c(z)\sim-\frac{me^2\omega_s}{2\hbar P_0}K_0\left[\frac{2m\omega_s z}{\hbar P_0}\right] . \tag{33c}$$

K_0 is a Bessel function.[13]

Note that the derivative of the effective potential in Eq. (33a) gives the semiclassical force.[14] For $\omega_{s\kappa}=\omega_s$ and neglecting the $\kappa^2/2$ term, the expression resulting from Eq. (33a) is finite for $z=0$,

$$R_e\Sigma_0^c(0)=-\frac{\pi me^2\omega_s}{4\hbar P_0} , \tag{33a'}$$

whereas the force at $z=0^+$ is given by

$$F_\perp(0)=+\left[\frac{me\omega_s}{\hbar P_0}\right]^2 . \tag{34}$$

D. Electron initially in a continuum state

Now take an electron initially in a continuum state of the δ-function potential. We shall report, for completeness, the expressions of the self-energy for an electron penetrating through a δ-function barrier at the surface. We want to find $\Sigma_\lambda(z)$ in the region $z>0$. The matrix elements needed in Eq. (9) are easily calculated, and the expression replacing Eq. (16') is

$$\Sigma_\lambda(z)=-\frac{me^2\omega_s}{2\hbar}\int_0^\infty d\kappa\frac{e^{-2\kappa z}}{m\omega_s/\hbar-2i\lambda\kappa}-f(z) , \tag{35}$$

where we have already set $P_0=0$ for simplicity. The function $f(z)$ is cumbersome, and not illuminating for the discussion. Note that the contribution from the ground-state term has cancelled out as before [see the discussion before Eq. (16')]. The first term on the right-hand side of Eq. (35) coincides with the classical image potential for large z. The result in Eq. (35) can also be compared with the results of Jonson[3] for a rectangular potential barrier. The first term in Eq. (35) is similar to Jonson's expression in the free-particle region, but our expression contains, in $\Sigma'_\lambda(z)$, two more complex oscillatory terms which arise from the δ-function barrier and from the recoil effect. We thus find some discrepancies, in comparison with Jonson's work, as we also noted in the discussion following Eq. (16').

IV. DISCUSSION

The expressions derived in the preceding section will be evaluated now, and their behavior will be discussed in terms of the parameter λ_0 that defines the strength of the δ-function potential, and for different electron-gas densities in the metal. We shall take the initial state of the electron to have zero momentum parallel with the surface, and shall set $\mathbf{P}_0=0$ in the expressions derived in Sec. III. The electron density in the metallic system, n_0, will be characterized by the so-called one-electron radius r_s, with $r_s=(3/4\pi n_0)^{1/3}$, and atomic units (a.u.) will be used hereafter, so that $\hbar=e=m=1$. The surface-plasmon frequency (or energy), in a.u., is given by $\omega_s=\omega_p/\sqrt{2}=(4\pi n_0/2)^{1/2}=(3/2r_s^3)^{1/2}$.

Figure 3 shows the spatial dependence of the two terms in the self-energy, Eqs. (17) and (18). The term Σ_{00} becomes more negative for increasing strength λ_0 of the potential, but it remains finite for $z=0$, contrary to the behavior of the classical image potential. The second term in the self-energy becomes positive for $z \gtrsim 2$ a.u. but it is smaller than $|\Sigma_{00}|$ for all z. The asymptotic limits given by Eqs. (21) are only approached for $z \gg 10$ a.u., and the larger λ_0 is, the faster this limit is approached. It is obvious from the expressions in Eqs. (17) and (18) that inclusion of the effect of dispersion of the surface plasmons reduces the absolute value of both contributions to the total self-energy.

Figure 4 shows the variation of the energy shift with the strength of the δ potential. The energy shift decreases until saturation is reached for large λ_0. Note that the result obtained invoking closure is similar to the exact energy shift, although slightly smaller. Furthermore, the contribution to the total energy shift due to the term $\Delta E_{0\lambda}$ in Eq. (22) is very small, below $\sim 5\%$ for all λ_0, and cancels for large λ_0.

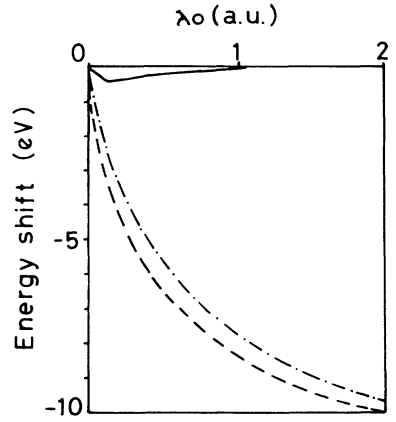

FIG. 4. Energy shift as a function of the strength of the potential, λ_0, for $r_s=3$ a.u. and $\omega_{s\kappa}=\omega_s$. Solid line: $\Delta E_{0\lambda}$, Eq. (24). Dashed-dotted line: ΔE_{00}, Eq. (23). Dashed line: ΔE_0^c, Eq. (26).

The energy shift is shown in Fig. 5 as a function of the electron-gas density parameter r_s. The dispersionless results are up to a factor of 2 smaller than the predictions based on the plasmon-pole dispersion model.[15] The effect of introducing a cutoff wave vector in the calculations is seen in Fig. 5 also, the resulting energy shifts being intermediate between those obtained neglecting dispersion in $\omega_{s\kappa}$, or using the plasmon-pole approximation to $\omega_{s\kappa}$. The self-energy obtained invoking closure is the lower curve shown in Fig. 5. Again, as in Fig. 4, this result is smaller than the exact self-energy.

In conclusion, we have analyzed, using a fully analytic

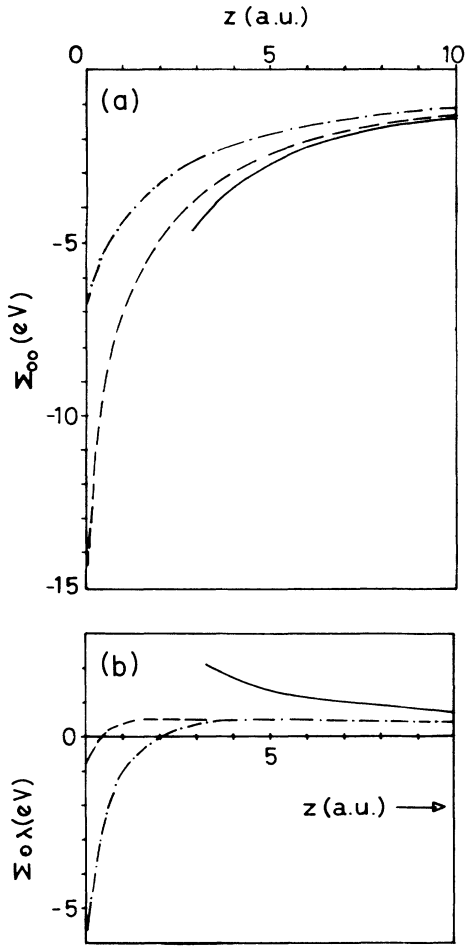

FIG. 3. Contributions (a) $\Sigma_{00}(z)$ and (b) $\Sigma_{0\lambda}(z)$ to the self-energy, Eqs. (17) and (18), with $\mathbf{P}_0=0$ and $\omega_{s\kappa}=\omega_s$, as a function of the distance z from the electron to the metal surface, for $r_s=2$ a.u. For $\lambda_0=2$ a.u. (dashed lines), and $\lambda_0=0.2$ a.u. (dashed-dotted lines). The asymptotic results, Eqs. (21) are also shown (continuous lines).

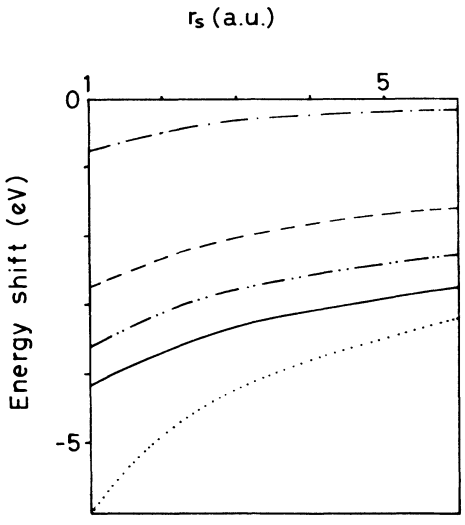

FIG. 5. Energy shifts, Eqs. (23), (24), and (26), as a function of the electron gas density, r_s, for $\lambda_0=0.2$ a.u. Solid line: ΔE_{00}, for $\omega_{s\kappa}=\omega_s$. Dashed-double-dotted line: ΔE_{00}, for $\omega_{s\kappa}=\omega_s$ and a cutoff $\kappa_c=\omega_p/v_F$. Dashed line: ΔE_{00}, using the surface-plasmon-pole model (Ref. 13) for $\omega_{s\kappa}$. Dashed-dotted line: $\Delta E_{0\lambda}$, for $\omega_{s\kappa}=\omega_s$. Dotted line: ΔE_0^c, Eq. (26).

model, the image potential appropriate for a tunneling electron. A reduction of the self-energy at close distances from the surface is predicted, compared with the classical result. Several topics are left for further elaboration, like the effect of virtual bulk excitations, and the study of the image potential in the region inside the potential barrier. With the formalism used in this work, one can analyze also the case of a potential barrier formed by piecewise constant potentials, and compare it with the calculations of Ref. 3. The width and height of the barrier against tunneling and the current resulting from a given applied electric field are importantly dependent on the self-energy function. The discussion of the current versus applied field characteristics of a barrier, based on our self-energy results, and implications of the approach for more realistic systems will be presented elsewhere.

ACKNOWLEDGMENTS

Partial financial support from the following organizations is recognized: the Spanish Comisión Asesora de Investigación Cientifica y Técnica, the U.S.—Spanish Comité Conjunto (CHN), the Division of Electrical Energy Systems, the U.S. Air Force Office for Scientific Research, under Interagency Agreement DOE No. 40-1604-85, and the U.S. Department of Energy, under Contract No. DE-AC 05-840R21400 with Martin Marietta Energy Systems Inc. One of us (P.M.E.) acknowledges support from the March Foundation and Iberduero S. A.

APPENDIX

The quantity $I(\kappa)$ in Eq. (18b) can be written as

$$I(\kappa)=\tfrac{1}{4}\int_{-\infty}^{\infty} d\lambda\,\lambda\frac{(\lambda+i\lambda_0)e^{i\lambda z}+(\lambda-i\lambda_0)e^{-i\lambda z}}{(\lambda^2+\lambda_0^2)[\lambda^2+(\lambda_0+\kappa)^2]\{\lambda^2+\lambda_0^2+[\mathbf{P}_0^2-(\mathbf{P}_0-\boldsymbol{\kappa})^2]+2m\omega_{s\kappa}/\hbar-i\delta\}}\ .$$

Setting $\mathbf{P}_0=\mathbf{0}$ for simplicity, and using the method of residues, one gets

$$I(\kappa)=-\frac{\pi\lambda_0 e^{-\lambda_0 z}}{\kappa(\kappa+2\lambda_0)(\kappa^2+2m\omega_{s\kappa}/\hbar)}-\frac{\pi e^{-(\lambda_0+\kappa)z}}{4\kappa(\lambda_0\kappa-m\omega_{s\kappa}/\hbar)}+\frac{\pi\exp-[(2m\omega_{s\kappa}/\hbar+\kappa^2+\lambda_0^2)^{1/2}z]}{4[(2m\omega_{s\kappa}/\hbar+\kappa^2+\lambda_0^2)^{1/2}-\lambda_0](\lambda_0\kappa-m\omega_{s\kappa}/\hbar)}\ .$$

The first term dominates for large z and finite κ and λ_0, whereas the first two terms contribute to the $\kappa\to 0$ limit.

[1]A. Hartstein and Z. A. Weinberg, Phys. Rev. B **20**, 1335 (1979); see also, A. Gras-Marti, P. M. Echenique, and R. H. Ritchie, Proc. Int. Symp. on Electrical Insulation, Washington (1986), p. 133.

[2]J. R. Manson and R. H. Ritchie, Phys. Rev. B **24**, 4867 (1981).

[3]M. Jonson, Solid State Commun. **33**, 743 (1980).

[4]E. Evans and L. D. Mills, Phys. Rev. B **8**, 4004 (1979).

[5]J. R. Manson, R. H. Ritchie, and T. L. Ferrell, Phys. Rev. B **29**, 1080 (1984); J. R. Manson and R. H. Ritchie, *ibid.* **29**, 1084 (1984); Nucl. Instrum. Methods B **2**, 422 (1984).

[6]J. R. Manson and R. H. Ritchie, Phys. Rev. Lett. **54**, 785 (1985).

[7]Note that one must include the contribution from bulk plasmon excitation, if the region $z<0$ (inside the medium) is to be treated adequately (see Ref. 2 for further comments). Here we are only interested in the calculation of the self-energy in the region $z>0$.

[8]The coupling coefficient for surface optical phonons of energy $\hbar\omega_\kappa$ is

$$\alpha_\kappa^2=(\pi e^2\hbar\omega_\kappa/A\kappa)[(\epsilon_0-1)/(\epsilon_0+1)-(\epsilon_\infty-1)/(\epsilon_\infty+1)]\ .$$

ϵ_0 is the static dielectric constant of the lattice, and ϵ_∞ the dielectric constant corresponding to high frequencies.

[9]Nieminen and Hodges, Phys. Rev. B **18**, 2568 (1978).

[10]P. M. Echenique and J. B. Pendry, Surf. Sci. **166**, 69 (1986).

[11]P. M. Echenique, R. H. Ritchie, N. Barberán, and J. Inkson, Phys. Rev. B **23**, 6486 (1981).

[12]P. M. Echenique and J. Pendry, J. Phys. C **8**, 2936 (1975).

[13]M. Abramowitz and I. A. Stegun, *Handbook of Mathematical Functions* (Dover, New York, 1972).

[14]N. Barberán, P. M. Echenique, and J. Viñas , J. Phys. C **12**, L111 (1979).

[15]One writes, in atomic units, $\omega_{s\kappa}=(\omega_s^2+\alpha\kappa+\beta\kappa^2+\kappa^4/4)^{1/2}$, with $\alpha=\sqrt{3/5}v_F\omega_s$, $\beta=0.0026+2.6798/r_s^{1.85}$. For comments on the values of the coefficients, see Ref. 11.